Second International Conference on CFD in the Minerals and Process Industries
CSIRO, Melbourne, Australia
6-8 December 1999

PARTICLE FLOW MODELLING ON SPIRAL CONCENTRATORS: BENEFITS OF DENSE MEDIA FOR COAL PROCESSING?

Brent W. MATTHEWS[1,2], Clive A.J. FLETCHER[1], Tony C. PARTRIDGE[2].

1. Centre for Advanced Numerical Computation in Engineering and Science
2. School of Mining Engineering
University of New South Wales, Sydney 2052, Australia

ABSTRACT

Spiral concentrators, used globally in the mineral processing industry, consist of an open trough that twists downward in helix configuration about a central axis. Particles fed to the top of the concentrator are separated radially on the basis of density and size as the slurry gravitates downward. To improve performance, CFD studies validated against experimental programs have been performed throughout the past decade. The CFD model development is now sufficiently advanced to predict reliably the free surface liquid and particle flow characteristics at concentrations where the particle-particle interactions are significant. The main focus of this paper is to examine computationally the potential of using dense media for coal processing by increasing the fluid density above that of water.

INTRODUCTION

The twisting open trough geometry of spiral concentrators is illustrated in Figure 1. Employed in the fine coal and heavy mineral processing industries, a slurry mix of fine (75 - 3000 μm) particles and water is fed to the top of the concentrator. As it gravitates downward, light suspended particles migrate outward by the centrifugal force whilst heavy particles settle in the flow (to regions of lower velocity) and travel inward toward the central column (Figure 2). Although segregation is supposed to occur on the basis of density, unintended size effects are also significant.

The first step in the CFD model development is the prediction of the liquid free surface profile as defined by the water depth across the trough. Isotropic turbulence models and the Volume of Fluid (VOF) free surface method underly the approach (Matthews *et al*., 1998a; Matthews *et al*., 1999). The particle flow has been examined by calculating the trajectories of individual particles based on the acting hydrodynamic forces (Matthews *et al*., 1998a) and by treating the particles as a continuum by using the dense gas kinetic theory and concept of granular temperature (Campbell, 1990; Matthews *et al*., 1998b).

This paper uses the continuum approach (Eulerian method) to examine the particle flow on coal spiral concentrators. The potential of using dense fluid media to highlight the role of material density during separation is emphasised. The important role of the particle-wall interactions is also addressed by considering the impact angles of colliding particles. The simulations have been conducted using FLUENT (v4.4) software.

Figure 1: Spiral concentrators in the processing plant.

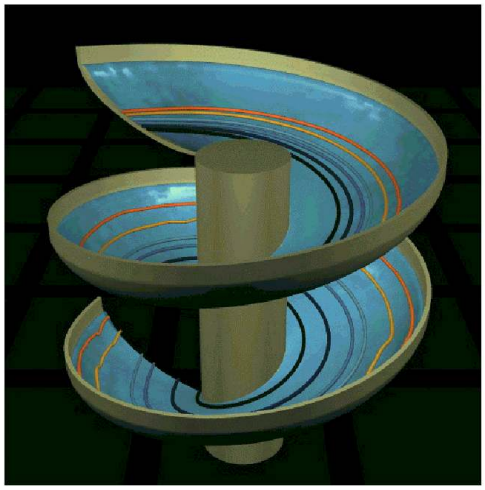

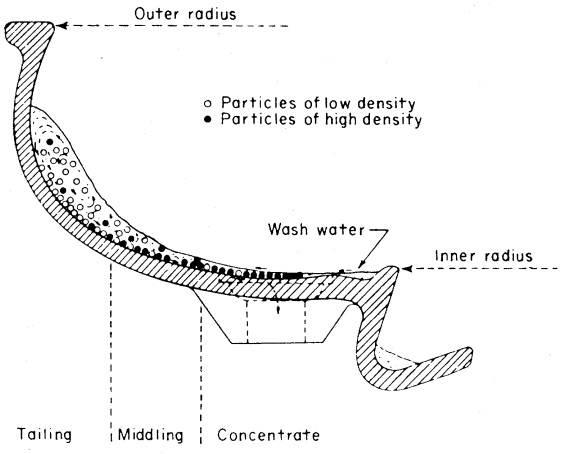

Figure 2: Operating mechanism: light particles in suspension travel outwards; heavy particles settle on the trough and slide inwards.

GEOMETRIC & FLOW CHARACTERISTICS

The number of turns on spiral concentrators varies typically from 5-7 and the trough width from 0.25-0.35m. The mainstream descent angle varies radially and is governed by the spiral pitch, defined as the vertical height loss per revolution of the helix. The LD9 coal-processing unit examined in this paper has a pitch of 0.273m, trough width of 0.28m and descent angles that reduce outward from 31-7°.

Water depths and mainstream velocities on the LD9 unit range respectively from 1-14 mm and 0.4-2.5 m/s which both increase outward across the trough. Consequently, laminar to progressively turbulent regimes exist. A secondary current normal to the main flow direction travels outward near the free surface and inwards near the trough base, is approximately an order of magnitude smaller than the mainstream component and is distinctly unsteady in nature. The detailed physics of the water flow are described in Matthews *et al*. (1999).

The particle flow on spiral concentrators is characterised by Stokes numbers that vary by several orders of magnitude (10^{-1}-10^{3}). In addition, particulate volume fractions decrease significantly outward across the trough from near maximum values in the inner region to dilute values at the outer radii (10^{0}-10^{-3}). Subsequently, the hydrodynamic, particle-particle and particle-wall interactions play important roles in the separation process whose relative importance varies for different particles and with radial positioning across the trough.

GOVERNING EQUATIONS

The Eulerian particulate flow is considered a two-phase problem where coupled equations are solved for both the water and particulate (single density and size) continua. The viscous and inertial stresses within the liquid phase are solved using the Navier-Stokes equations and isotropic k-ε turbulence model. The particulate equations are similar to the Navier-Stokes but where the molecular viscosity varies as a by-product of the flow itself. By assuming a fixed free surface profile, the continuity equation for phase q (either water or particle phase) is:

$$\frac{\partial}{\partial t}\left(\alpha_q \rho_q\right)+\nabla\cdot\left(\alpha_q \rho_q \mathbf{u}_q\right)=0 \tag{1}$$

where α_q and ρ_q are respectively the volume fraction and material density of phase q. The momentum conservation equations for the fluid (f) and particulate (p) phases are respectively given by:

$$\frac{\partial}{\partial t}\left(\alpha_f \rho_f \mathbf{u}_f\right)+\nabla\cdot\left(\alpha_f \rho_f \mathbf{u}_f \mathbf{u}_f\right)=-\alpha_f \nabla p_f + \nabla.\tau_f + \alpha_f \rho_f \mathbf{g} + K_{pf}\left(\mathbf{u}_p-\mathbf{u}_f\right) \tag{2}$$

$$\frac{\partial}{\partial t}\left(\alpha_p \rho_p \mathbf{u}_p\right)+\nabla\cdot\left(\alpha_p \rho_p \mathbf{u}_p \mathbf{u}_p\right)=-\alpha_p \nabla p_f - \nabla p_p + \nabla.\tau_p + \alpha_p \rho_p \mathbf{g} - K_{pf}\left(\mathbf{u}_p-\mathbf{u}_f\right) \tag{3}$$

where P is the pressure, K_{pf} is the particle-fluid momentum exchange coefficient, and the stress tensor (τ) is defined by:

$$\tau_q=\alpha_q \mu_q\left[\nabla\mathbf{u}_q+\left(\nabla\mathbf{u}_q\right)^T\right] \tag{4}$$

The frictional transfer of momentum due to long-term particle contacts is ignored and the remaining stresses arising from the particle inertia and particle-particle collisions are solved using the dense gas kinetic theory (Campbell, 1990). Closure models are expressed in terms of the mean square of the instantaneous deviation from the local mean particulate velocity, defined as the granular temperature, T. The granular temperature field is solved by (Ding and Gidaspow, 1990):

$$\frac{3}{2}\frac{\partial}{\partial t}\left(\rho_p \alpha_p T\right)+\frac{3}{2}\nabla\cdot\left(\rho_p \alpha_p \mathbf{u}_p T\right)= \left(-p_p I+\tau_p\right):\nabla\mathbf{u}_p+\nabla.\Gamma_T\nabla T-\gamma_T+\phi_p \tag{5}$$

where the terms on the right-hand-side of (5) represent respectively, the generation of T, its diffusion from high to low T, dissipation due to inelastic particle collisions, and viscous energy exchange from the particulate to fluid phases.

The mutual exchange of momentum between the liquid and particulate continua is simulated using the measurements of terminal velocities of particles in settling and fluidised beds (Syamlal *et al*., 1993). The turbulent dispersion of particles is based on the Tchen theory where coefficients, correlation functions, and the particulate viscosity are given in terms of the fluid turbulence field (Simonin, 1991). The particles are assumed to suppress the fluid turbulence through the inclusion of source terms in the fluid turbulence transport equations (Elghobashi and Abou-Arab, 1983).

PARTICLE-WALL INTERACTION

In the Lagrangian analysis of Matthews *et al*. (1998a), impulse equations describing the interaction between a smooth spherical particle and smooth wall were used to determine the translational velocities immediately after impact of individual particles (Matsumoto and Saito, 1970). The presence or absence of sliding at the contact interface between the particle and wall determined two types of collision. A collision without sliding took place when the following condition was satisfied (Matsumoto and Saito, 1970; Sommerfeld, 1992):

$$\left|u_p-\left(\frac{D_p}{2}\omega_p\right)\right|<\frac{7}{2}\phi_0\left(1+e\right)v_p \tag{6}$$

where ω_p is the particle angular velocity and u_p and v_p are respectively the particle tangential and normal velocity components relative to the wall. Due primarily to low particle impact angles, sliding collisions were assumed to dominate so that the particle rotation played a minor role and was ignored (Matthews *et al*., 1998a). By assuming values for the restitution coefficient (e) and static friction coefficient (φ_0) of 0.8 and and 0.2 respectively, (6) reveals that sliding contacts will occur for impact angles of < 21-38° depending upon the value of ω_p.

By using the terminal velocity of particles processed on the LD9 unit, it is found that impact angles could be expected to vary substantially from <1-78° decreasing radially outward as u_p increases (Matthews, 1999). Within

the Eulerian framework, two separate boundary conditions are prescribed at the interface between the particle and wall surfaces which lead to simulation of non-sliding contacts and, conversely, sliding in the absence of friction. These represent the two limits during impact in the Lagrangian treatment and generate wall shear stresses that, respectively, are maximum and minimum values.

NUMERICAL PROCEDURE & PROPERTIES

The Volume of Fluid (VOF) method (Hirt and Nichols, 1981) was used to determine the free surface location of the water flow at 6 m^3/hr. To optimise computational efficiency, the water and air components of the single fluid flow were solved on a grid representing a small 36° sector of the spiral domain (Figure 3). Results were fed progressively from near the outlet to the inlet until steady state conditions had been reached. Excellent predictions of the water depths and primary and secondary velocities have been obtained (Matthews *et al*., 1999). Details of the numerical procedure and boundary conditions used are described in Matthews *et al*. (1998a).

The water depths defined the location of the free surface boundary and were used to create a second computational domain on which the coupled Eulerian particulate-water flow was solved (Figure 4). This grid consisted of 20 x 43 x 11 cells in the mainstream, cross-stream and depth-wise directions respectively and on which the free surface location remained fixed.

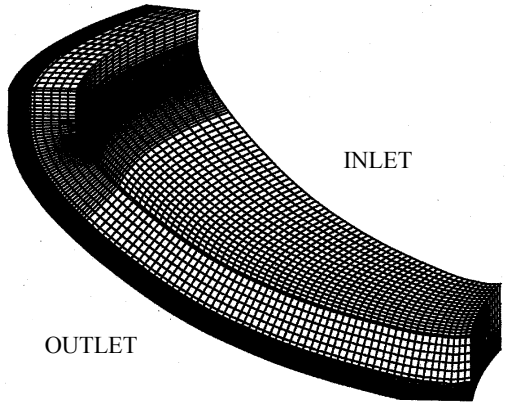

Figure 3: Computational domain for the fluid flow on the LD9 concentrator.

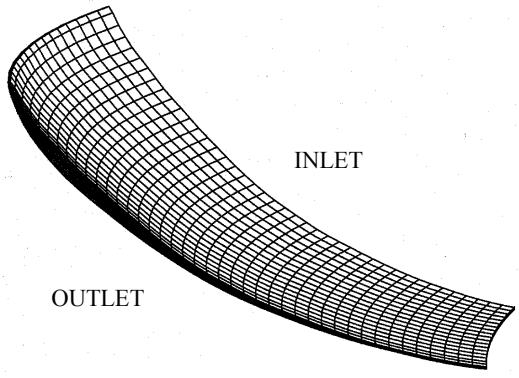

Figure 4: Computational domain for the Eulerian particulate-water flow on the LD9 concentrator.

The volume fraction and mainstream velocity of the particulate phase were arbitrarily specified to give the desired flow rate. Time-steps of 0.0005-0.001s were used with 700-1500 time-steps needed to achieve steady flow conditions for each solution on the grid. Residuals were reduced to below 10^{-5} to conserve mass to within 0.02%. Typically, 50-100 cycles of transferring results from near the outlet to the inlet were needed to reach the steady state. The numerical details are described in Matthews (1999).

The water phase is assumed to have constant physical properties of ρ_f = 1000 kg/m^3 and μ_f = 0.0009 kg/ms. Refuse particles (ρ_p = 2440 and 2650 kg/m^3) and coal (1200 and 1450 kg/m^3) are examined in this paper. The particulate continua are examined separately and have single and constant ρ_p and diameter (D_p), but μ_p that varies as a function of the granular temperature. Dense fluid media above that of water are examined by adding magnetite (ρ_p = 5200 kg/m^3) to the flow and treating the suspension as a viscous fluid with μ_f defined by that given in Shook and Roco (1991).

RESULTS

The particle analysis has been restricted to a dilute feed rate of 0.3% by mass relative to the water phase that is two orders of magnitude smaller than the industrial rate. This has been done for two reasons. The first is to replicate numerically the experiments of Holtham (1990) which demonstrated that the radial positioning of particles was not significantly affected by the particulate loading. Second, as the free surface location needs to be assumed in the model, corrections to the depth as predicted by the VOF method are not required because the particles do not modify the depth at the dilute feed rate. This preserves the fully predictive nature of the model.

Using the frictionless wall surface, the cumulative weight percent of refuse particles outward across the LD9 trough is presented in Figure 5. The equivalent measurements are also shown (Holtham, 1990). Approximately 50% of the 75 μm particles accumulate in the innermost region with the remainder moving to the outermost radii. As occurs in practice, the 530 μm particles all settle on the trough and slide toward the central column. The generally excellent predictions of the radial distributions of 75 and 530 μm grains is related to the low impact angles of particle-wall collisions where sliding contacts can be assumed.

The 1400 μm distribution is poorly predicted using the frictionless wall, as impact angles are sufficiently high across the trough for sliding contacts not to occur. Accordingly, the converse and second wall boundary condition of non-sliding at the contact interface has been used to predict the particulate radial distributions (Figure 6). Although a small proportion of 1400 μm grains accumulates toward the central column, most particles independently of size move to the outermost regions (Figure 6).

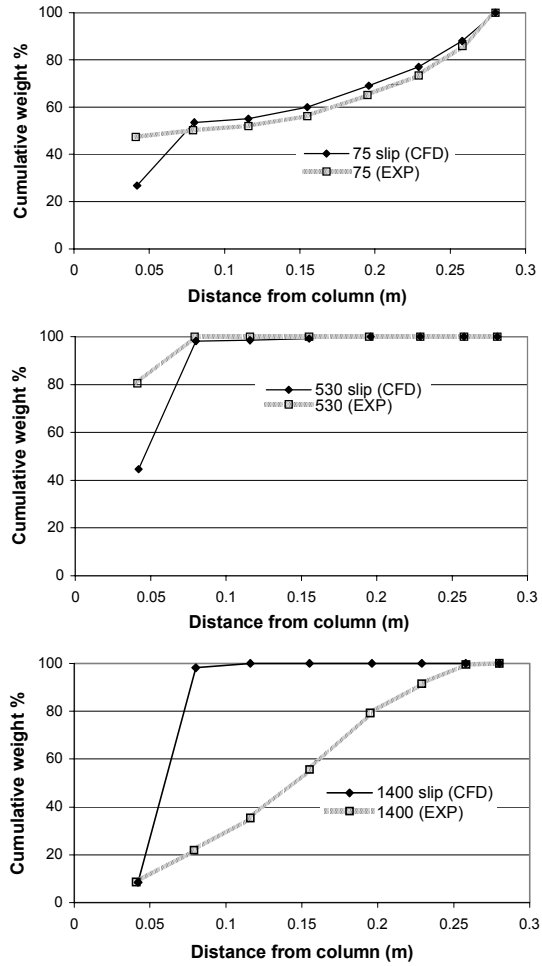

Figure 5: Measured radial distributions of 75, 530 and 1400 μm refuse particles and those simulated using the frictionless wall in the Eulerian analysis.

The outward movement of particles using the non-sliding wall is related to the generation of high velocity gradients and thus granular temperatures in the near-wall region (Campbell, 1990). This in turn leads to significant particulate pressures that overcome the weight of particles, keeping them suspended to move outward by the centrifugal force (Matthews *et al*., 1998b). The generation of high velocity gradients is caused by the specification of zero velocity at the wall that is clearly inappropriate for the fine to medium sized particles and indeed the 1400 μm particles across the entire trough width.

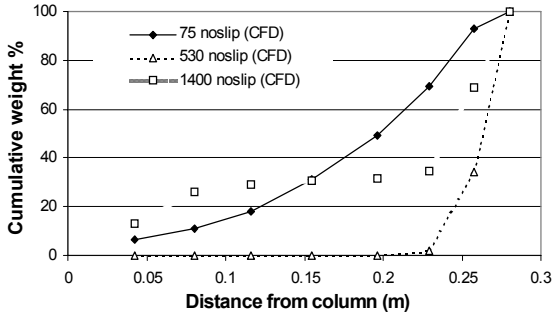

Figure 6: Simulated radial distributions of 75, 530 and 1400 μm refuse particles using the non-slip wall in the Eulerian analysis.

When particles move further outward, the contact interface between the particle and wall surfaces is more likely to encounter slip because as the particles are travelling faster their impact angles are reduced. Although the inception of slip is difficult to quantify due to uncertainties in estimating the settling velocity, the two wall boundary conditions are used simultaneously for the 1400 μm examination. Specifically, the frictionless wall is employed at radial distance greater than 0.2 m from the central column, and the non-slip wall at less than 0.2 m. Satisfactory agreement with the measurements is then found (Figure 7).

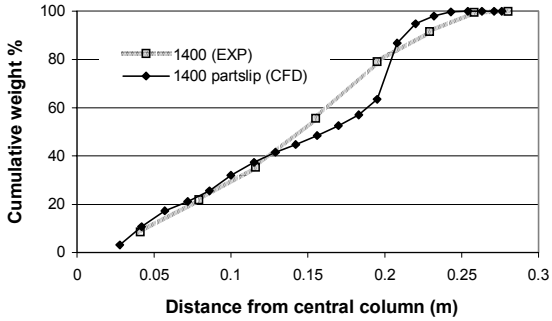

Figure 7: Measured radial distributions of 1400 μm refuse particles and those simulated using the combined frictionless and non-slip wall in the Eulerian analysis.

By subdividing the trough into eight streams, Holtham (1990) measured the volume concentrations of refuse particles across the LD9 concentrator (Figure 8). The equivalent simulations using the frictionless wall for 75 and 530 μm and the combined wall types for 1400 μm are also given. The measured fractions reduce from near maximum possible value (0.6) where particles are tightly packed to minimum values discernible by the procedure of 0.0001. The model has generally captured the radial concentrations accurately.

The simulated and invalidated radial distributions of thermal coal (ρ_p = 1450 kg/m^3) are given in Figure 9. It is found that although the 75 and 1400 μm particles largely move as intended to the outer regions (Figure 2), a significant portion of mid-size grains (530 μm) accumulate at the inner radii. The reduced particulate weight with respect to the refuse particles implies that even the frictionless wall generates pressures that can overcome the weight of 1400 μm grains, keeping them mainly in suspension.

On spiral concentrators used for coal processing, separation ideally occurs as heavy (high ρ_p) particles settle on the trough and light (low ρ_p) particles remain suspended (Figure 2). However, because particles over a wide range of diameters ($D_p \approx$ 100 – 1500 μm) and comparatively smaller range of densities (1200 – 2650 kg/m^3) are processed, separation inevitably occurs by size also. Indeed, characteristic values of the Stokes number indicate that the relative behaviour is influenced mainly by size (Matthews, 1999). This is reflected by the radial distributions of refuse and coal particles (Figures 5, 6, 7 and 9).

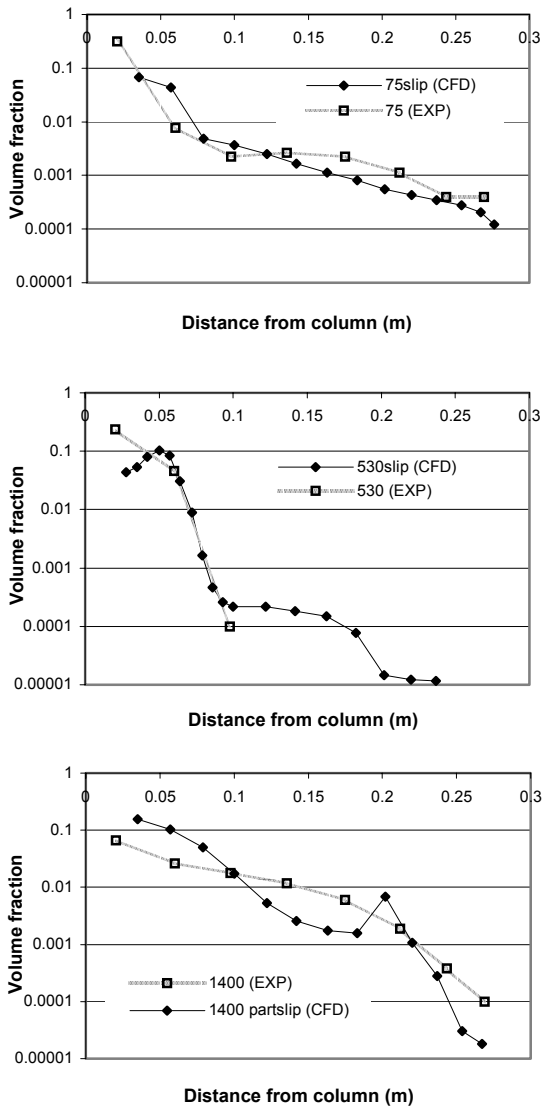

Figure 8: Comparison be tween measured and simulated volume fractions of 75 (top), 530 (mid) and 1400 μm (bottom) refuse particles.

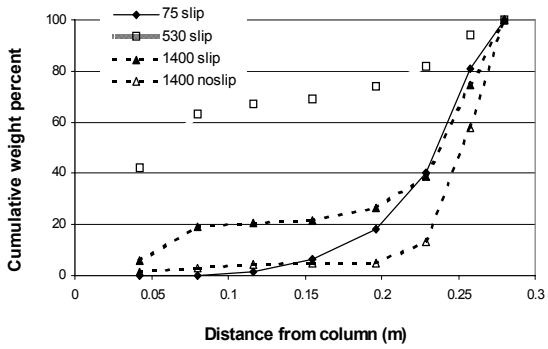

Figure 9: Simulated radial coal distributions using the frictionless wall for 75, 530 and 1400 μm particles and non-slip wall for 1400 μm grains.

The potential benefit of using dense media on spiral concentrators has been examined numerically by adding magnetite to increase the fluid density. On the LD9 unit, simulations have been conducted with ρ_f = 1400 kg/m^3 (c.f. 1000 kg/m^3 for water). The radial distributions are given in Figure 10. It is found that unlike the water medium, coal particles regardless of size move to the outer regions. In addition, there is a single definitive cut at 0.23m from the central column that largely separates the desired product and refuse material. However, this is far from the central column and there is little scope for particles of ρ_p between 1450 and 2650 kg/m^3 to be separated as the reject material moves into the mid and outer trough regions.

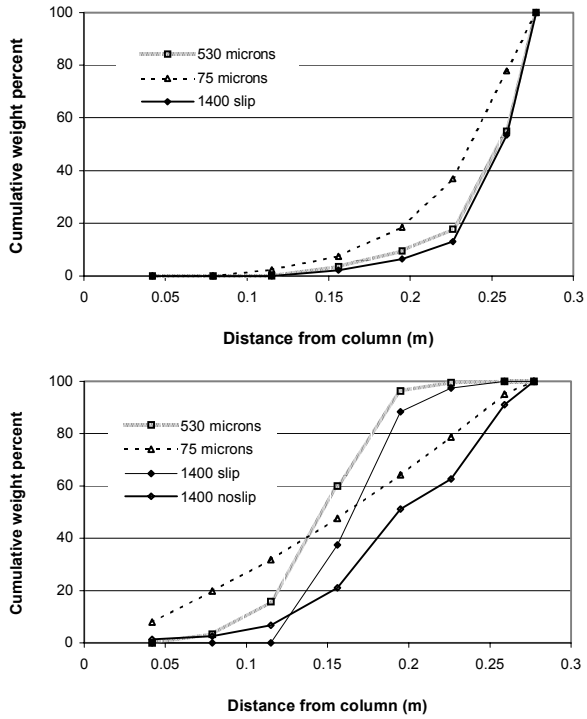

Figure 10: Predicted radial distributions on the LD9 unit using a dense medium (1400 kg/m^3) for coal (top) and refuse quartz grains (bottom). 75 and 530 μm particles assume a "slip" wall.

Accordingly, to preclude the outward movements of refuse material, an original prototype proposed by the authors has been investigated. Steeper transverse slopes of the trough at the inner radii as well as a smaller pitch of 0.183m (to reduce the centrifugal force) have been used. The radial distributions by assuming a frictionless wall are given in Figure 11. It is found that separation based on ρ_p differences has been enhanced whilst the unintended size effects have been minimised.

It must be stressed that the simulations in Figure 11 have assumed sliding particle-wall collisions that are invalid for larger particles whose impact angles are above the critical angles delineating sliding and non-sliding contacts. Because non-sliding contacts lead to outward movement and preferentially occur for more dense refuse material for a given particle size, they should be avoided in the design process. Non-sliding results in high particulate pressures and uplifting shear-slip (Saffman, 1965) and rotation-slip (Rubinow and Keller, 1961) forces that keep particles in suspension. The Lagrangian analysis, by accounting for the particle-wall friction, reveals that if sliding contacts can be induced, the particles travel generally faster than the water flow. This largely negates the unintended uplifting mechanisms (Matthews, 1999).

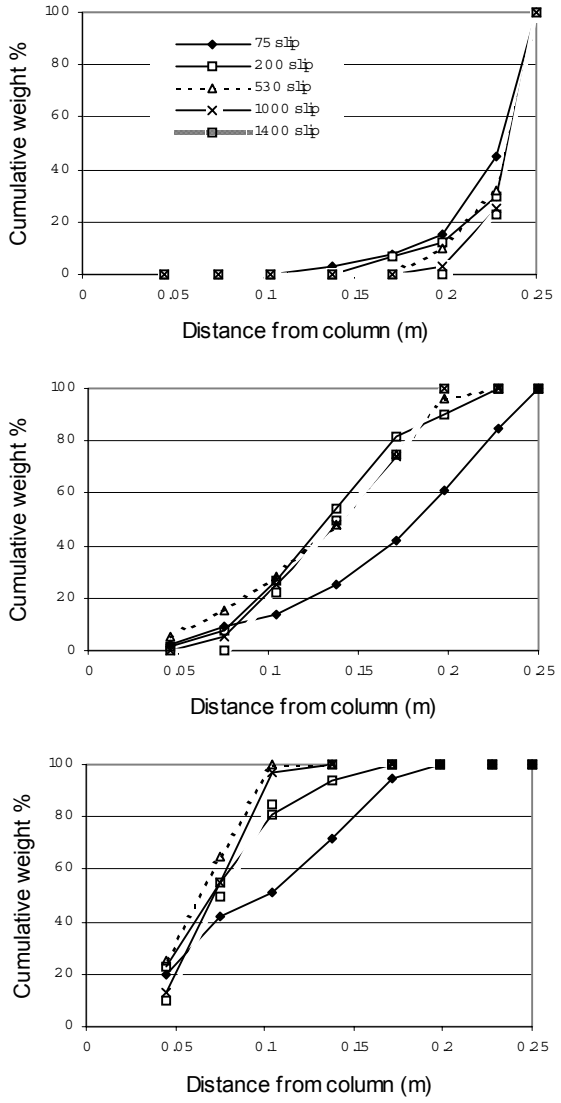

Figure 11: Predicted radial distributions on the original unit using a dense medium (1200 kg/m^3) for particles of D_p = 75-1400 µm and with ρ_p = 1200 kg/m^3 (top), 1750 kg/m^3 (mid) and 2650 kg/m^3 (bottom).

To induce sliding contacts the pitch of the concentrator and hence the mainstream velocity could be increased to reduce the collision angle. As the centrifugal forces would also be greater, steeper transverse slopes may be required to preclude refuse material from moving outward once sliding can be achieved. In addition, the density of the carrier fluid that now offers an extra degree of freedom in the design process could be reduced, and operations involving narrow feed size distributions may prove to be beneficial.

CONCLUSION

The Eulerian approach using the concept of granular temperature and dense gas kinetic theory has been applied successfully to predict the radial distributions of particles on spiral concentrators. This is in spite of severely violating the continuum assumption in the depth-wise direction of the flow (Matthews, 1999). The particle-wall behaviour is particularly important in governing the flow rheology where the appropriate conditions have been employed by considering the impact angles of colliding particles. Because of the difficulties in distinguishing between the particle size and density effects on spiral concentrators used for coal processing, this paper reveals potential benefit in raising the density of the carrier fluid above that of water.

REFERENCES

CAMPBELL, C.S., (1990), "Rapid granular flows", *Ann. Rev. Fluid Mech*., **22**, 57-92.

DING, J., GIDASPOW, D., (1990), "A bubbling fluidisation model using kinetic theory of granular flow", *AIChE J*., **36(4)**, 523-538.

ELGHOBASHI, S.E. and ABOU-ARAB, T.W., (1983), "A two-equation turbulence model for two-phase flows", *Phy. Fluids A*, **26**, 931-938.

HIRT, C.W. and NICHOLDS, B.D., (1981), "Volume of Fluid (VOF) method for the dynamics of free boundaries", *J. Comp. Phy*., **39**, 201-225.

HOLTHAM, P.N., (1990), "The fluid flow patterns and particle motion on spiral separators", Ph.D. Thesis, University of New South Wales, Australia.

MATSUMOTO, S. and SAITO, S., (1970), "Monte Carlo simulation of horizontal pneumatic conveying based on the rough wall model", *J. Chem. Eng. Japan*, **3(2)**, 223-230.

MATTHEWS, B.W., (1999), "Computations of spiral concentrator flows", Ph.D. Thesis, University of New South Wales, Australia.

MATTHEWS, B.W., FLETCHER, C.A.J, PARTRIDGE, A.C., (1998a), "Computational simulation of fluid and dilute particulate flows on spiral concentrators", *App. Math. Model*., **22**, 965-979.

MATTHEWS, B.W., HOLTHAM, P.N., FLETCHER, C.A.J., GOLAB, K, PARTRIDGE, A.C., (1998b), "Computational and experimental investigation of spiral concentrator flows", *Proc. XIII Int. Coal Prep. Congress*, Brisbane, Australia, 965-979.

MATTHEWS, B.W., FLETCHER, C.AJ, PARTRIDGE, A.C., VASQUEZ, S., (1999), "Computations of curved free surface water flow on spiral concentrators", ASCE *J. Hyd. Eng*.**,** to appear in November issue.

RUBINOW, S.I. and KELLER, J.B., (1961), "The transverse force on a spinning sphere moving in a viscous fluid", *J. Fluid Mech*., **11**, 447-459.

SAFFMAN, P.G., (1965), "The lift on a small sphere in a slow shear flow", *J. Fluid Mech*., **22**, 385-400.

SHOOK, C.A. and ROCO, M.C., (1991), *Slurry flow principles and practice*, Butterworth-Heinemann, U.S.A.

SIMONIN, O., (1991), "Prediction of the dispersed phase turbulence in particle-laden jets", *Proc. 4th Symp. Gas-solid flows*, ASME. FED, **121**, 197-206.

SOMMERFELD, M., (1992), "Modelling of particle-wall collisions in confined gas-particle flows", *Int. J. Multiphase Flow*, **18(6)**, 905-926.

SYAMLAL, M., ROGERS, W., O'BRIEN, T.J., (1993), "MFIX Documentation: Vol. 1, Theory Guide, DOE/METC-9411004, NTIS, DE9400087, National Technical Information Service, Springfield, VA, USA.